



RESEARCH ARTICLE – MATERIAL SCIENCE (MISCELLANEOUS)

Calcium Phosphate Coatings with Controlled Micro/Nano-Structures for Endothelial Cells Viability

Adil Elrayah^{1*}, Ke Duan², Xiong Lu³, Xiaobo Lu², Jie Weng²

¹Medicine College, Karary University, Omdurman 12304, Sudan

²Key Laboratory of Advanced Technologies of Materials, School of Chemistry, Southwest Jiaotong University, Chengdu, 610031, China

³Department of Bone and Joint Surgery, Affiliated Hospital of Southwest Medical University, Luzhou, Sichuan 646000, China

* Corresponding author E-mail: adil.karary@karary.edu.sd

Article Info.	Abstract
<p>Article history:</p> <p>Received 30 March 2024</p> <p>Accepted 22 May 2024</p> <p>Publishing 30 June 2024</p>	<p>Hydroxyapatite (HA) scaffolds produced by the accumulation of HA fibers were separately treated hydrothermally in three calcium phosphate solutions to form coatings of different micro/nano-structures. Different micro/nano-structure and morphologies have been regulated on the surface of treated HA scaffolds. Plate-like, flower-like morphology was obtained with solution 1 (Ca-sufficient), i.e., ratio: Ca/Ca=1%; Ca/P=1.67. Full coatings (flower-like) morphology treated after Cu-doped coating solution 2 (Cu/(Cu+Ca) = 5%; ratio: (Cu+Ca)/P = 1.67). Furthermore, partial coatings (flower-like) morphology fabricated with solution 3 (Ca-deficient and Cu-replacement), i.e., ratio: Ca/Ca=0.95%; Ca/P=1.58. The results showed the effect of hydrothermal coatings on HA scaffolds. Cultured human endothelial cells spread and proliferated better on the treated HA scaffolds than on the uncoated scaffolds, suggesting a potential effect of calcium phosphate surface morphology on endothelial cell response. Thus, it can provide an appropriate micro/nano-structure approach supporting angiogenesis capacity, which is a necessity to accelerate the time of bone healing and regeneration.</p>

This is an open-access article under the CC BY 4.0 license (<http://creativecommons.org/licenses/by/4.0/>)

Publisher: Middle Technical University

Keywords: Hydroxyapatite; Micro/Nano-Structure; Scaffolds; Coating; Endothelial Cell.

1. Introduction

Hydroxyapatite (HA, $\text{Ca}_{10}(\text{PO}_4)_6(\text{OH})_2$) is the common mineral found in vertebral bones [1], and widely used for bone repair because of its similarity to human bone mineral [2, 3]. In addition to the chemical constitution, an ideal surface micro/nano-structure is also desirable for the development of bioactive materials [4]. In particular, Ca cations in the HA structure can be substituted by several metal cations, e.g., Na^+ , Ag^+ , Mg^{2+} , Ni^{2+} , Sr^{2+} , Fe^{3+} and La^{3+} [5]. Various techniques have been reported for surface coating or modification of calcium phosphate scaffolds, such as precipitation, sol-gel, solid-state, hydrothermal, and biomimetic methods [6-8].

Of these, the hydrothermal process offers advantages such as fast production, relative technical simplicity, and high crystallinity of the product [7]. In this method, the pH and ion concentrations (e.g., Ca^{2+} , PO_4^{3-}) are key parameters affecting the morphology, and crystal size of the coating formed [9]. However, few studies have investigated modulating the micro/nano-structure of calcium phosphate coatings deposited on HA scaffolds. Most HA scaffold modifications in the hydrothermal method used inorganic [10] or organic [11] modifiers. Our previous study reported controlling the nanostructures of calcium phosphate coatings hydrothermally deposited on HA scaffolds by introducing organic crystal growth modifiers (i.e., hexacarboxylic acid) [6]. As many organic modifiers (e.g., hexacarboxylic acid) are generally not present in the human body, their use might involve concerns of safety and clinical practicality. Recently, also we prepared micro/nano-structure on HA scaffolds by hydrothermal treatment with the assistance of organic modifier ions (copper)[10]. This work investigated the effect of Cu^{2+} on the HA scaffolds coating using the hydrothermal method. However, it did not consider the impact of the identical hydrothermal condition without an inorganic modifier (copper ions) on HA scaffolds.

Addressing the micro/nano-structure of HA scaffolds with hydrothermal coatings and their effects on endothelial cell (EC) viability is still unclear. In contrast, methods of modifying the surface morphology of HA scaffolds with only physiologically present substances may be preferred. Furthermore, angiogenesis formation has an essential role in physiological bone defect repair [12]. Consequently, the interactions between endothelial cells (EC) and orthopedic biomaterials need to be investigated for achieving optimum clinical outcomes. Several studies

Nomenclature & Symbols

HA	Hydroxyapatite	EC	Endothelial Cell
Ca(NO ₃) ₂	Calcium Nitrate	Na ₂ HPO ₄	Disodium Phosphate

Examined EC interactions with HA granules or nanoparticles and reported favorable responses, such as normal morphology and activated gene expression related to angiogenesis [13, 14].

In this study, a hydrothermal treatment was used to prepare calcium phosphate coatings with controlled micro/nano-structures on HA scaffolds. The physiological effects of the coatings with and without copper ions have been studied. Furthermore, the adhesion of EC on the surfaces was studied in vitro, and their formation mechanisms were examined.

2. Materials and Methods

2.1. Material HA scaffolds preparation

An HA slurry was prepared by mixing 20 g of HA powder (Kelong Chemical, Chengdu, Sichuan, China) with 100 mL of sodium alginate solution (3 wt.%) [15]. The slurry was transferred in a syringe and injected into a CaCl₂ solution (0.2 mol/L) to form cross-linked fibers. The fibers were immediately collected and packed in molds to create cylindrical scaffolds. They were dried at 70 °C for 10 h and sintered at 1200 °C for 2 h [15] to form scaffolds (size: $\Phi 5 \times 10$ mm). Three calcium phosphate coatings, termed Ca_{9.5}-HA, Ca₁₀-HA, and Cu_{0.5}Ca_{9.5}-HA were separately prepared as shown in Fig. 1.

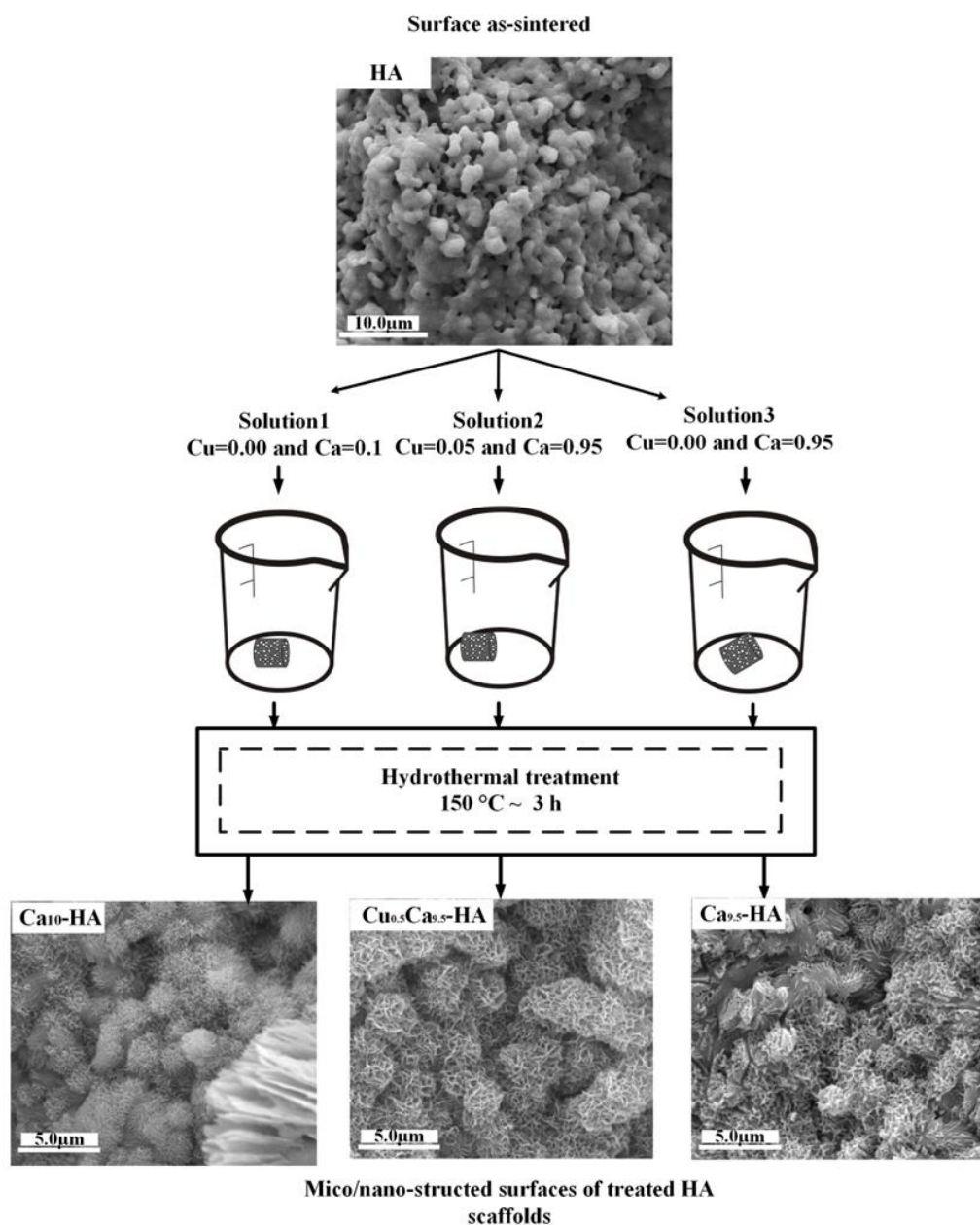


Fig. 1. Schematic illustration of the hydrothermal coatings process and the resulting scaffold surface morphologies

Three solutions were prepared for coating preparation as shown in Table 1. The first solution (Solution 1), comprising 0.1 mol/L $\text{Ca}(\text{NO}_3)_2$ and 0.06 mol/L Na_2HPO_4 (Ca/P molar ratio=1.67), was used for the preparation of the coatings on the Ca_{10} -HA scaffolds. The second one (Solution 2), containing 0.095 mol/L $\text{Ca}(\text{NO}_3)_2$, 0.005 mol/L $\text{Cu}(\text{NO}_3)_2$, and 0.06 mol/L Na_2HPO_4 ((Cu+Ca)/P=1.67; and Cu/(Cu+Ca)=5%), was used to prepare the coatings on $\text{Cu}_{0.5}\text{Ca}_{9.5}$ -HA scaffolds. The third one (Solution 3), containing 0.095 mol/L $\text{Ca}(\text{NO}_3)_2$ and 0.06 mol/L Na_2HPO_4 (Ca/P=1.58), was used to prepare the coatings on $\text{Ca}_{9.5}$ -HA scaffolds. Each solution was adjusted to $\text{pH } 2.50 \pm 0.05$ by dropwise addition of HNO_3 ; then, 1 g/30mL of urea ($\text{CH}_4\text{N}_2\text{O}$) was added to the solution [16]. Then, the as-sintered HA scaffolds were immersed separately in the three solutions and transferred to an autoclave. The autoclave was heated to 150 °C, maintained at this temperature for 3 h, and then cooled to room temperature, as shown in Fig. 1. During this hydrothermal treatment, urea decomposed to generate ammonia, thereby increasing the pH and inducing calcium phosphate crystallization. Finally, the samples were retrieved, rinsed with deionized water, and dried (80 °C, 3 h) [6].

Table 1. Chemical components (% weights ± 0.05) of hydroxyapatite (HA) solutions

Samples	Ca	Cu	P	Ca/P	(Cu+Ca)/P	Cu/(Cu+Ca)
Ca_{10} -HA	39.86	0	18.4	1.67	1.67	0.00
$\text{Cu}_{0.05}\text{Ca}_{9.5}$ -HA	37.87	3.15	18.4	1.67	1.67	0.05
$\text{Ca}_{9.5}$ -HA	37.87	0	18.4	1.67	1.58	0.00

2.2. In vitro cell culture preparation

Human ECs (Sichuan University, Chengdu, Sichuan, China) were seeded on scaffolds (pre-sterilized at 140°C, 3 h) at 1×10^5 cells/scaffold, and cultured (37 °C, 5% CO_2 , 95% relative humidity) in 80% of α -minimum essential medium (MEM; Gibco, Carlsbad, CA, USA) supplemented with 10% fetal bovine serum, and 1% penicillin/streptomycin for 5 d. Alamar blue (AB) assays were performed to determine the proliferation of ECs. The medium was discarded and replaced with fresh medium with 10% AB reagent (Invitrogen, Carlsbad, CA, USA). After incubation at 37 °C for 4 h, the optical densities at 570 and 600 nm were measured (μ Quant microplate reader, Bio-Tek Instruments, Winooski, USA). Wells with as-sintered samples were used as the control, and empty wells served as the blank. Data were expressed as a percentage of AB reduction, which correlates with the number of viable cells.

3. Result and Discussion

3.1. Microstructure formation on HA scaffold

The surface microstructure of the un-coated and coated scaffolds was investigated by means of Scanning electron Microscope (SEM). Fig. 2 shows un-coated scaffolds, which are covered with smooth crystalline grains, including micro/nano-crystals and pores with an average crystal diameter of $2.1 \pm 1.0 \mu\text{m}$.

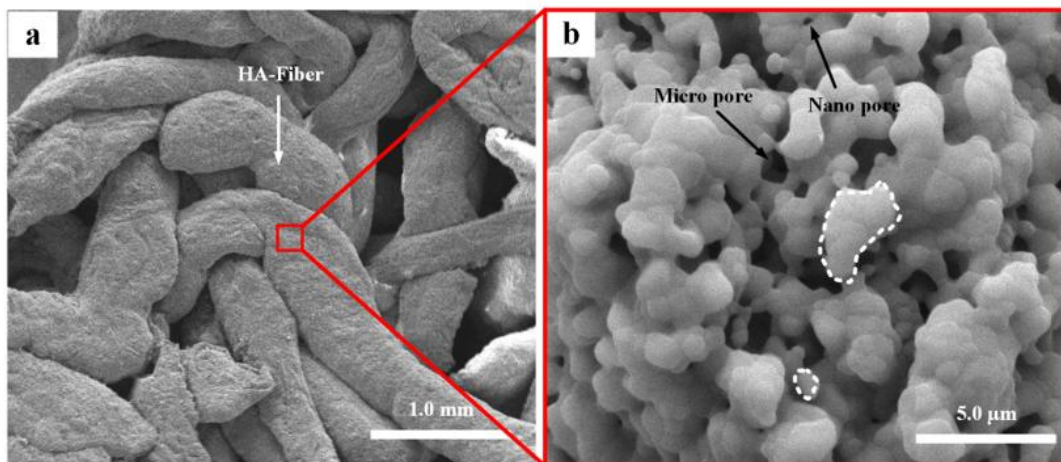


Fig. 2. SEM micrographs of (a, b) typical morphologies of as-sintered HA

After hydrothermal treatment using Ca/P solutions (Fig. 3), the morphology of treated scaffolds was substantially changed compared to the un-coated ones. Figs. 3a and b illustrated plate-like micro-crystals on the surface of Ca_{10} -HA scaffold (crystals diameter: $46.45 \pm 20 \mu\text{m}$), aggregating into flower-like micro/nano-structures (crystal's diameter is: $2.21 \pm 0.5 \mu\text{m}$). The results indicated that the sufficient calcium in solution 1 could affect the size of crystal formations on the Ca_{10} -HA scaffold compared to others. Fig. 3 demonstrated the improvement of coatings on the $\text{Cu}_{0.5}\text{Ca}_{9.5}$ -HA scaffold surfaces. Scattered flower-like crystals (diameter approximately $3.4 \pm 1.4 \mu\text{m}$) and silkworm-like crystals (diameter $8.5 \pm 2.1 \mu\text{m}$) were observed, as shown in Fig. 3c. The results indicated the effect of Cu in the hydrothermal solution, which could facilitate full coatings on the $\text{Cu}_{0.5}\text{Ca}_{9.5}$ -HA scaffold surfaces (Fig. 3c). Fig. 3d showed $\text{Ca}_{9.5}$ -HA scaffolds with partial coatings compared to $\text{Cu}_{0.5}\text{Ca}_{9.5}$ -HA scaffolds.

The coating using Cu-replacement solutions could change the scaffold morphology from smooth (as in uncoated scaffolds) to flower-like (crystal diameter $2.4 \pm 0.8 \mu\text{m}$) and silkworm-like (crystal size $4.03 \pm 1.3 \mu\text{m}$). Moreover, the black rows in Fig.3d demonstrated the partial coating area on the scaffold.

In general, the growth of calcium phosphate crystals depends on the solution pH, temperature, Ca/P ratio, and the presence of ions or biomolecules [17].

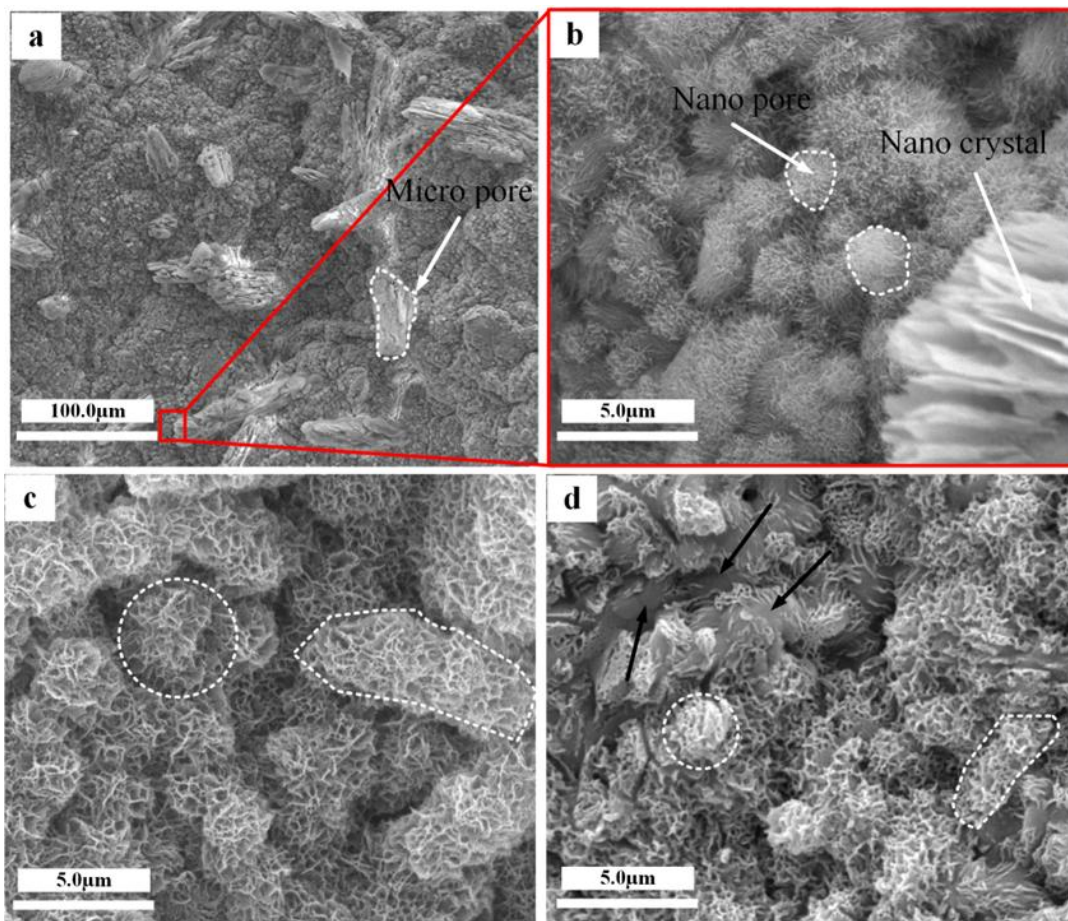


Fig. 3. SEM characterized the coated scaffolds hydrothermally with micrographs of (a, b) Ca10-HA, (c) Ca9.5-HA, and (d) Cu0.05Ca9.5-HA

Based on the above results, we predicted the mechanism of coatings behind calcium phosphate deposited on the treated HA scaffolds. When as-sintered HA scaffolds were immersed into solutions under the initial acidic conditions ($\text{pH} = 2.5$), Ca^{2+} and PO_4^{3-} probably dissolved into the surrounding solution from the scaffolds. With an increase in the reaction temperature, the solution became increasingly alkaline because of urea decomposition. The dissolved ions may accelerate crystal nucleation around the surface of the scaffolds; thus, the process promotes the Ca/P micro/nano-structure deposited on the surface of the HA scaffolds. A similar experiment was carried out by Ye et al. [8], who used hydrothermal conditions to generate HA micro-whiskers in Ca/P ceramics. The whisker growth mechanism involved a dissolution-redeposition procedure, which specifically indicated that β -TCP in the ceramic matrix simply dissolved into calcium and phosphate ions, then redeposited and shaped HA micro-whiskers under hydrothermal treatment.

The overall results suggested that the micro/nano-structures deposited on the treated scaffolds are attributed to the effect of the solution compositions. The surfaces of the scaffolds may trigger the EC viability response and may enhance the angiogenesis capacity as well as bone healing and regeneration.

To further characterize the surface composition of the treated HA scaffolds, X-ray diffraction (XRD, PANalytical X'Pert PRO, Philips, Netherlands, $\text{CuK}\alpha$, 35 mA, 45 kV) was used. The XRD patterns (Fig. 4) illustrated the treated scaffolds which had a compose of apatite phase similar to the phase that constituted an initial HA scaffold. Furthermore, no significant difference was observed for Cu0.5Ca9.5-HA with respect to the addition of copper ions, which may be attributed to the strong diffraction peak of the substrate and lower presence of copper.

3.2. In vitro evaluation of HA and treated scaffolds

The EC morphologies on treated HA scaffolds were investigated by SEM. Fig.5 demonstrated a sustainable increase of EC proliferation on HA scaffolds with increasing culture time. Fig.5a illustrated that the cells had distributed in an area of $0.17 \mu\text{m}$ on the HA scaffold (uncoated). Fig. 5b showed that the EC were spread in an area of $0.48 \mu\text{m}$ on the Ca10-HA scaffold. Furthermore, Fig.5c illustrated the spread of EC on the Ca9.5-HA scaffold, with more adhering cells covering an area of $0.35 \mu\text{m}$. Fig.5d showed that EC were dispersed in an area of $0.87 \mu\text{m}$ on the Cu0.5Ca9.5-HA scaffold.

The results indicated that the $\text{Cu}_{0.5}\text{Ca}_{9.5}\text{-HA}$ scaffold has a higher presence of EC spread compared with the others, and the less EC spread was observed on HA scaffold (un coated). These findings indicated that the treated scaffolds can support EC adhesion and spread better than the uncoated scaffold, which may be attributed to their structures [18, 19]. Furthermore, the presence of Cu could not only influence the physical-chemical properties of scaffolds, but also support EC adhesion and spread on them [20].

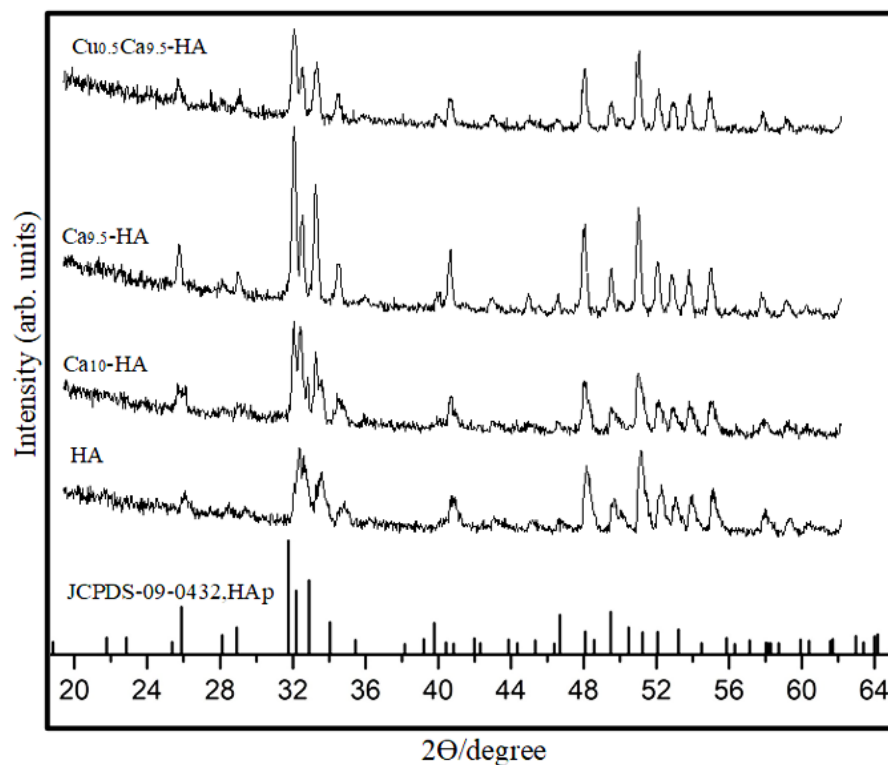


Fig. 4. XRD spectra of as-sintered HA, Ca10-HA, Ca9.5-HA, Cu0.5Ca9.5-HA, and standard spectra of (HAp)

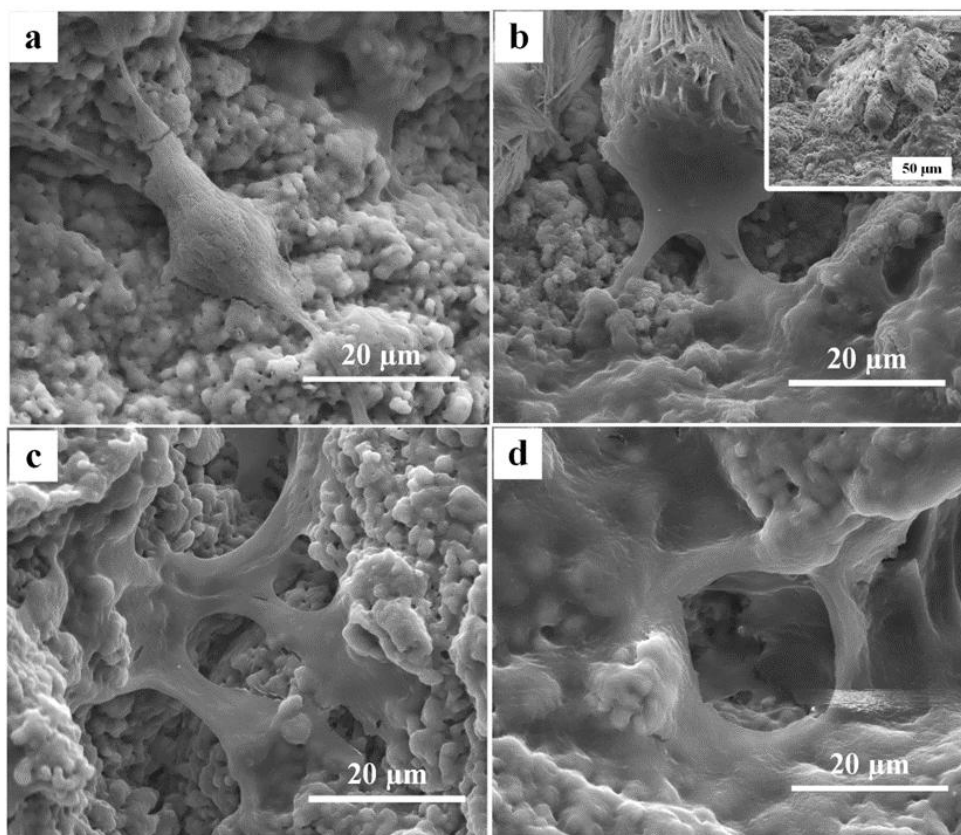


Fig. 5. SEM images illustrating endothelial cell (EC) culture after five days: (a) as-sintered HA scaffold; (b) Ca10-HA scaffold; (c) Ca9.5-HA scaffold; and (d) $\text{Cu}_{0.5}\text{Ca}_{9.5}\text{-HA}$ scaffold

3.3. EC Viability of HA and treated scaffolds

Fig. 6 illustrates Alamar Blue (AB) assays characterized on days 1, 3, and 5. The difference between groups occurred on the 3rd and 5th days. The t-test value showed a significant difference between groups ($p < 0.05$). Within the same group, a different observation was illustrated in the EC viability rate during culture times. The uncoated HA scaffolds were used as controls in this experiment. After culturing, the EC viability on the 1st day showed that the scaffolds Ca10-HA and Ca9.5-HA exhibited insignificant differences compared with the control ($p > 0.05$). The results found that the Ca10-HA (Ca-sufficient) affected the EC viability response compared with Ca9.5-HA (Ca-deficient), which may imply that the key factor of this effect is the micro/nano-structures growth on the Ca10-HA scaffold. The EC viability response on Cu_{0.5}Ca 9.5-HA scaffold after 5th day was significantly different compared with the other groups ($p < 0.05$). The results indicated that the Cu_{0.5}Ca9.5-HA scaffold obtained a higher EC viability compared with the other scaffolds. Thus, referring to the desired micro-nano-structure on the scaffold, which was prepared with a Cu-doped hydrothermal coating solution. Previous study reported that the copper ions as a trace element in the human body can play a vital role in promoting endothelial cells migration and the angiogenic formation [21]. The overall results suggested that the Cu_{0.5}Ca_{9.5}-HA scaffolds features may have benefits for angiogenesis capacity. Thus, this gives the scaffolds a good choice as bone substitute scaffolds, especially for use in bone healing and regeneration.

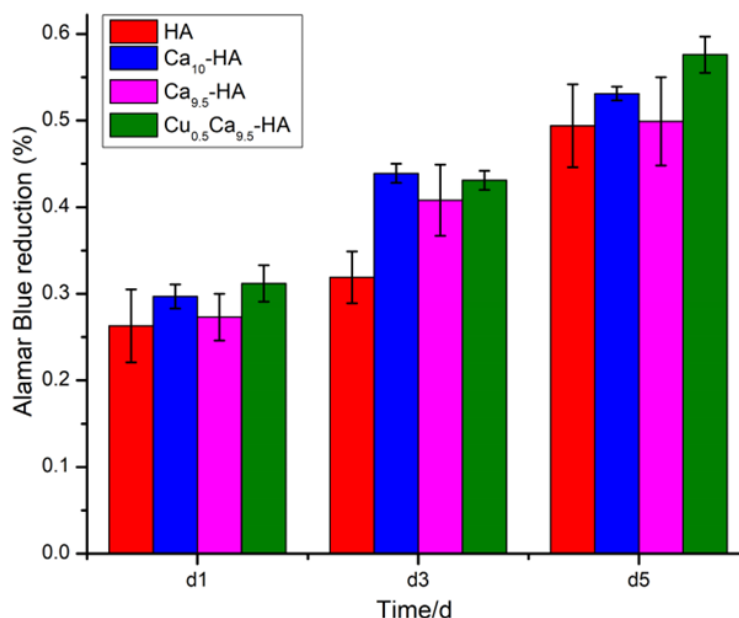


Fig. 6. The bar chart illustrated EC viability during cell culture

4. Conclusion

- Calcium phosphate coatings with controlled micro/nano-structures were successfully grown on HA scaffolds using the hydrothermal method.
- The results indicated that Solution 1 (Ca-sufficient) improved different morphologies (micro/nano-structure) on the Ca10-HA scaffold compared with the morphology of the Ca9.5-HA scaffold treated with Solution 2 (Ca-deficient).
- The results indicated that Cu-doped hydrothermal coatings could improve the structure of Cu_{0.5}Ca_{9.5}-HA scaffold and influence the full coatings on scaffold compared with Ca_{9.5}-HA scaffold (without copper).
- The results found that the treated Cu_{0.5}Ca_{9.5}-HA and Ca10-HA scaffolds are more conducive to EC viability compared with the other scaffolds.
- The overall results suggested that the micro/nano-structure on the scaffolds may provide an appropriate approach for angiogenesis capacity.

Conflicts of Interest

The authors declare no conflicts of interest.

Acknowledgments

The National Key Research and Development Program of China grant number (2016YFB0700803), the National Natural Science Foundation of China grant number (51572228) and Karary University, Sudan, funded this research.

References

- [1] N. Eliaz and N. Metoki, "Calcium Phosphate Bioceramics: A Review of Their History, Structure, Properties, Coating Technologies and Biomedical Applications," *Materials*, vol. 10, no. 4, 2017, <https://doi.org/10.3390/ma10040334>.
- [2] T. M. Sridhar, U. K. Mudali, and M. Subbaiyan, "Preparation and characterisation of electrophoretically deposited hydroxyapatite coatings on type 316L stainless steel," *Corrosion Science*, vol. 45, no. 2, pp. 237-252, 2003, [https://doi.org/10.1016/S0010-938X\(02\)00091-4](https://doi.org/10.1016/S0010-938X(02)00091-4).

- [3] S. S. A. Abidi and Q. Murtaza, "Synthesis and Characterization of Nano-hydroxyapatite Powder Using Wet Chemical Precipitation Reaction," *Journal of Materials Science & Technology*, vol. 30, no. 4, pp. 307-310, 2014, <https://doi.org/10.1016/j.jmst.2013.10.011>.
- [4] K. Batebi, B. Abbasi Khazaei, and A. Afshar, "Characterization of sol-gel derived silver/fluor-hydroxyapatite composite coatings on titanium substrate," *Surface and Coatings Technology*, vol. 352, pp. 522-528, 2018, <https://doi.org/10.1016/j.surfcoat.2018.08.021>.
- [5] M. Othmani, H. Bachoua, Y. Ghandour, A. Aissa, and M. Debbabi, "Synthesis, characterization and catalytic properties of copper-substituted hydroxyapatite nanocrystals," *Materials Research Bulletin*, vol. 97, pp. 560-566, 2018, <https://doi.org/10.1016/j.materresbull.2017.09.056>.
- [6] D. Xiao, T. Guo, F. Yang, G. Feng, F. Shi, J. Li, et al., "In situ formation of nanostructured calcium phosphate coatings on porous hydroxyapatite scaffolds using a hydrothermal method and the effect on mesenchymal stem cell behavior," *Ceramics International*, vol. 43, no. 1, pp. 1588-1596, 2017, <https://doi.org/10.1016/j.ceramint.2016.10.023>.
- [7] M. M. Taheri, M. R. Abdul Kadir, T. Shokuhfar, A. Hamlekhan, M. Assadian, M. R. Shirdar, et al., "Surfactant-assisted hydrothermal synthesis of Fluoridated Hydroxyapatite nanorods," *Ceramics International*, vol. 41, no. 8, pp. 9867-9872, 2015, <https://doi.org/10.1016/j.ceramint.2015.04.061>.
- [8] X. Ye, C. Zhou, Z. Xiao, Y. Fan, X. Zhu, Y. Sun, et al., "Fabrication and characterization of porous 3D whisker-covered calcium phosphate scaffolds," *Materials Letters*, vol. 128, pp. 179-182, 2014, <https://doi.org/10.1016/j.matlet.2014.04.142>.
- [9] J. Qin, Z. Zhong, and J. Ma, "Biomimetic synthesis of hybrid hydroxyapatite nanoparticles using nanogel template for controlled release of bovine serum albumin," *Mater Sci Eng C Mater Biol Appl*, vol. 62, pp. 377-83, May 2016, <https://doi.org/10.1016/j.msec.2016.01.088>.
- [10] A. Elrayah, W. Zhi, S. Feng, S. Al-Ezzi, H. Lei, and J. Weng, "Preparation of Micro/Nano-Structure Copper-Substituted Hydroxyapatite Scaffolds with Improved Angiogenesis Capacity for Bone Regeneration," *Materials (Basel)*, vol. 11, no.9, Aug 23 2018, <https://doi.org/10.3390/ma11091516>.
- [11] S. Guang, F. Ke, and Y. Shen, "Controlled Preparation and Formation Mechanism of Hydroxyapatite Nanoparticles under Different Hydrothermal Conditions," *Journal of Materials Science & Technology*, vol. 31, no.8, pp. 852-856, 2015, <https://doi.org/10.1016/j.jmst.2014.12.013>.
- [12] S. M. Chim, J. Tickner, S. T. Chow, V. Kuek, B. Guo, G. Zhang, et al., "Angiogenic factors in bone local environment," *Cytokine Growth Factor Rev*, vol. 24, no. 3, pp. 297-310, Jun 2013, <https://doi.org/10.1016/j.cytogfr.2013.03.008>.
- [13] M. S. Laranjeira, M. H. Fernandes, and F. J. Monteiro, "Response of monocultured and co-cultured human microvascular endothelial cells and mesenchymal stem cells to macroporous granules of nanostructured-hydroxyapatite agglomerates," *J Biomed Nanotechnol*, vol. 9, no. 9, pp. 1594-606, Sep 2013, <https://doi.org/10.1166/jbn.2013.1664>.
- [14] S. Pezzatini, R. Solito, L. Morbidelli, S. Lamponi, E. Boanini, A. Bigi, et al., "The effect of hydroxyapatite nanocrystals on microvascular endothelial cell viability and functions," *J Biomed Mater Res A*, vol. 76, no.3, pp. 656-63, Mar 1 2006, <https://doi.org/10.1002/jbm.a.30524>.
- [15] G.-S. Lee, J.-H. Park, U. S. Shin, and H.-W. Kim, "Direct deposited porous scaffolds of calcium phosphate cement with alginate for drug delivery and bone tissue engineering," *Acta biomaterialia*, vol. 7, no.8, pp. 3178-3186, 2011, <https://doi.org/10.1016/j.actbio.2011.04.008>.
- [16] Z. S. Stojanovic, N. Ignjatovic, V. Wu, V. Zunic, L. Veselinovic, S. Skapin, et al., "Hydrothermally processed 1D hydroxyapatite: Mechanism of formation and biocompatibility studies," *Mater Sci Eng C Mater Biol Appl*, vol. 68, pp. 746-57, Nov 01 2016, <https://doi.org/10.1016/j.msec.2016.06.047>.
- [17] X. X. Wang, L. Yang, H. Liu, Q. Chen, D. Q. Xiao, and J. G. Zhu, "Optical Properties of ZnS:Co+Cr Nanocrystals Synthesized by a Low Temperature Hydrothermal Process," *Journal of Inorganic Materials*, vol. 29, no.10, pp. 1049-1054, 2014.
- [18] A. Magnaudeix, J. Usseglio, M. Lasgorceix, F. Lalloue, C. Damia, J. Brie, et al., "Quantitative analysis of vascular colonisation and angiogenesis in porous silicon-substituted hydroxyapatite with various pore shapes in a chick chorioallantoic membrane (CAM) model," *Acta Biomaterialia*, vol. 38, pp. 179-189, 2016, <https://doi.org/10.1016/j.actbio.2016.04.039>.
- [19] X. Li, C. A. van Blitterswijk, Q. Feng, F. Cui, and F. Watari, "The effect of calcium phosphate microstructure on bone-related cells in vitro," *Biomaterials*, vol. 29, no.23, pp. 3306-3316, 2008, <https://doi.org/10.1016/j.biomaterials.2008.04.039>.
- [20] F. E Imrie and J. M. S. Skakle, "Preparation of Copper-Doped Hydroxyapatite with Varying x in the Composition Ca₁₀(PO₄)₆Cu_xO_yH_z," *Bioceramics Development and Applications*, vol. 3, 2013, DOI: 10.4172/2090-5025.S1-005.
- [21] M. A. Saghiri, A. Asatourian, J. Orangi, C. M. Sorenson, and N. Sheibani, "Functional role of inorganic trace elements in angiogenesis- Part II: Cr, Si, Zn, Cu, and S," *Crit Rev Oncol Hematol*, vol. 96, no.1, pp. 143-55, Oct 2015, <https://doi.org/10.1016/j.critrevonc.2015.05.011>.